Spallation reactions – physics and applications

A. Kelić, M. V. Ricciardi, K.-H. Schmidt
Gesellschaft für Schwerionenforschung, GSI, Planckstr. 1, D-64291 Darmstadt, Germany

Abstract. Spallation reactions have become an ideal tool for studying the equation of state and thermal instabilities of nuclear matter. In astrophysics, the interactions of cosmic rays with the interstellar medium have to be understood in detail for deducing their original composition and their production mechanisms. Renewed interest in spallation reactions with protons around 1 GeV came up recently with the developments of spallation neutron sources. The project of an accelerator-driven system (ADS) as a technological solution for incinerating the radioactive waste even intensified the efforts for better understanding the physics involved in the spallation process.
Experiments on spallation reactions were performed for determining the production cross sections and properties of particles, fragments and heavy residues. Traditional experiments on heavy residues, performed in direct kinematics, were limited to the direct observation of long-lived radioactive nuclides and did not provide detailed information on the kinematics of the reaction. Therefore, an innovative experimental method has been developed, based on inverse kinematics, which allowed to identify all reaction residues in-flight, using the high-resolution magnetic spectrometer FRS of GSI, Darmstadt. It also gives direct access to the reaction kinematics. An experimental campaign has been carried out in a Europe-wide collaboration, investigating the spallation of several nuclei ranging from ^{56}Fe to ^{238}U. Complementary experiments were performed with a full-acceptance detection system, yielding total fission cross sections. Recently, another detection system using the large-acceptance ALADIN dipole and the LAND neutron detector was introduced to measure light particles in coincidence with the heavy residues.
Another intense activity was dedicated to developing codes, which cover nuclear reactions occurring in an ADS. The first phase of the reaction is successfully described by a sequence of quasi-free nucleon-nucleon collisions with an intra-nuclear-cascade code. Most of the salient features observed in the residual nuclide distributions are determined by the later de-excitation stage of the reaction due to the different possible de-excitation paths like evaporation of nucleons, light charged particles and intermediate-mass fragments, fission and multi-fragmentation.

Introduction

Nuclear collisions at relativistic and ultra-relativistic energies have first been studied using cosmic rays as projectiles and nuclear-track detectors for visualising the reaction products (see e.g. ref. [1]). As the typical signatures of collisions between nucleons or other particles and nuclei at these high energies, a large number of particles and fragments were registered. The observed patterns, schematically shown in Figure 1, suggested to name this type of reaction “spallation”. Later, accelerators were able to deliver well-defined beams, and the detection technique developed considerably. Spallation reactions gained increasing interest by their importance in different fields of physics and by their applications in technology. Therefore, much effort has been invested in experiments on the properties of residues and particles produced in spallation reactions. At the same time, the theoretical understanding improved, and powerful nuclear-reaction codes were developed.

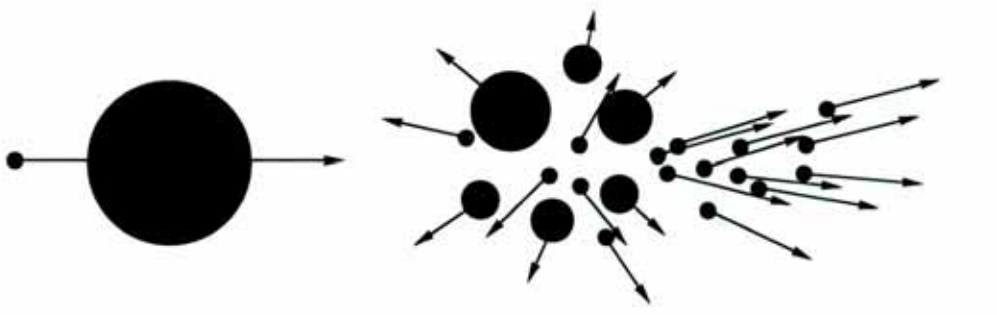

Figure 1. Schematic drawing of a typical spallation reaction. (Figure taken from ref. [2])

In this contribution we will give a review on the applications of spallation reactions in technology and basic science, the experimental techniques to study the spallation process, the empirical knowledge, the theoretical understanding and the models developed to understand and to simulate the different stages of this complex reaction type.

Applications

The applications of spallation reactions in technology and basic science are manifold. They comprise astrophysics, production of rare-isotope beams, production of neutrons in spallation neutron sources and accelerator-driven systems as well as investigations of heated nuclear matter.
In astrophysics, there are mainly two fields of interest. When exploring the sources of heavy nuclei, which are detected as cosmic-ray particles, it is important to understand the nuclear reactions they encounter in collisions with mostly hydrogen in the interstellar medium. But spallation at relative velocities around 0.5 c was also discussed as a possible nucleosynthesis mechanism within a supernova [3].
Spallation reactions have proven to be very efficient in producing rare isotopes. Three prominent facilities are listed in table 1. The rare isotopes produced in a thick target by spallation with proton beams of energies between 200 MeV and 1.4 GeV are extracted by the ISOL technique. ISOLDE [4] is operating very successfully at CERN for several decades already, TRIUMF [5] has become operational recently and EURISOL [6] is the European project for a next-generation large-scale ISOL-based secondary-beam facility.

Table 1. Present and planned secondary-beam facilities based on spallation reactions.

Facility	Proton beam	Output
ISOLDE CERN	≤ 1.4 GeV	Rare isotopes
TRIUMF Vancouver	200 MeV	Rare isotopes, neutrons, pions, muons
EURISOL (Project)	1 GeV	Rare isotopes

Spallation reactions also deliver a large number of neutrons. Therefore, spallation neutron sources are the heart of several neutron facilities. Table 2 lists a few prominent facilities and compares them with the high-flux fission reactor at the Institute Laue-Langevin in Grenoble [7]. While SINQ [8] at the Paul-Scherrer Institute in Villigen provides a continuous neutron flux like a reactor, the neutron beams from ISIS [9] at the Rutherford laboratory and from SNS [10] at the Oak Ridge National Laboratory are characterised by a time structure, which allows determining the energy of the interacting neutron by a time-of-flight measurement. The low neutron energies required for investigations of condensed matter are obtained by moderation of the primary spallation neutrons. The n_TOF facility [11] at CERN, which is dedicated to experiments on interactions of neutrons with nuclei, provides neutrons up to much higher energies.

Table 2. Technical parameters of some prominent neutron sources.

Type	Facility	Proton beam	Neutron energy	Time structure	Neutron flux
Fission reactor	ILL Grenoble	---	cold, thermal, epithermal	continuous	$1.3\ 10^{15}$ n/(cm^2 s)
Spallation neutron source	SINQ Villigen	500 MeV, 1.8 mA		continuous	$1.1\ 10^{14}$ n/(cm^2 s)
	ISIS Rutherford	800 MeV, 200 µA		50 Hz, 400 ns	
	SNS Oak Ridge	1 GeV, 1.4 mA		60 Hz, 695 ns	
	n_TOF CERN	200 GeV/c	thermal – several 100 MeV	0.42 Hz, 6 ns	

A very peculiar application of a spallation neutron source is envisaged in the project of the accelerator-driven system. A subcritical fission reactor is supplemented with a proton accelerator, which provides the additional neutron flux to make the reactor critical and thus operational. The schematic lay out of an ADS is shown in Figure 2. Due to this extended concept, the reactor is more flexible in its operation

conditions. This is an important advantage, if this reactor is used for incinerating radioactive waste material, e.g. minor actinides with very long half-lives left over from conventional fission reactors. The first demonstration prototype of an ADS is being developed at Mol, Belgium under the name Myrrha [12].

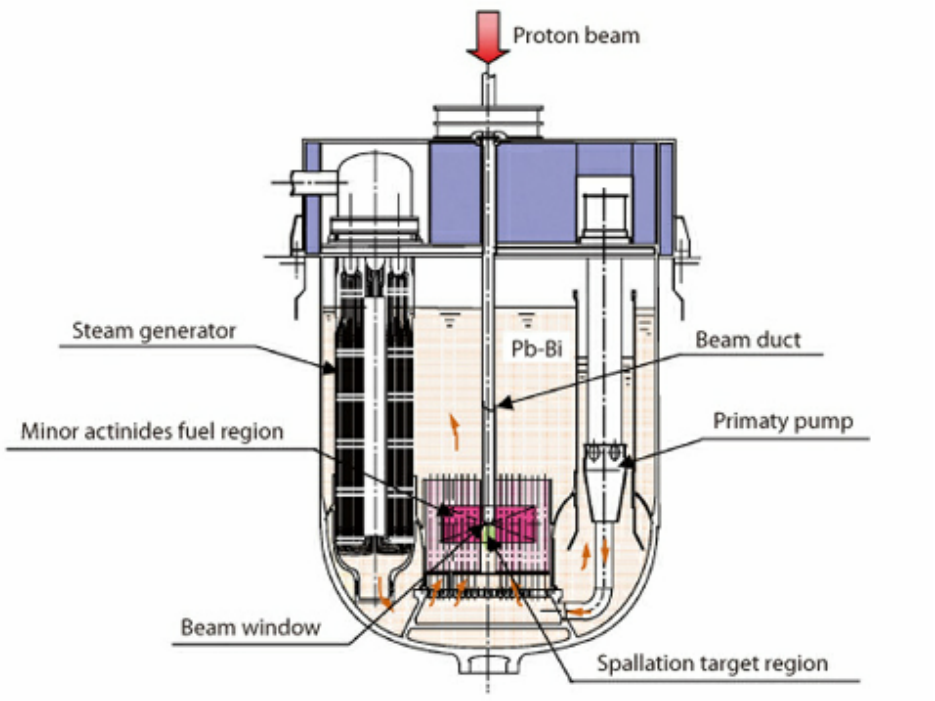

Figure 2. Schematic layout of an accelerator-driven system, consisting of a fission reactor and a spallation neutron source, which is fed by a ≈ 1 GeV proton beam. (Figure taken from ref. [13]).

Spallation reactions are also an ideal tool to heat up nuclear matter. The incoming high-energetic particle (in most cases a proton) induces intrinsic excitations, which are thermalized very fast. Thus, spallation reactions have intensively been used to study the equation of state of nuclear matter, see e.g. ref. [2], in particular at very high temperatures.

Experiments

Direct kinematics

Traditionally, experiments on spallation reactions have been performed by bombarding the material of interest by the high-energetic light projectiles. Neutrons and light charged particles leave the target with sufficiently high kinetic energies to be recorded by kinematical detectors.

The double-differential neutron cross section is characterized at high energies by a forward-directed component, which originates from the first nucleon-nucleon collisions, before the energy introduced by the projectile is distributed over the whole target nucleus and the system is thermally equilibrated. The neutrons emitted after equilibration are emitted isotropically with a Maxwell distribution and thus dominate the low-energy part of the spectrum. An example of an experiment performed at SATURNE is shown in Figure 3.

The energy spectra of light charged fragments are restricted to much lower energies. They show only slightly enhanced energies in forward direction. This anisotropy reveals that the emission starts, before full thermal equilibrium is reached. Figure 4 shows an example from an experiment performed with the PISA set-up in Jülich.

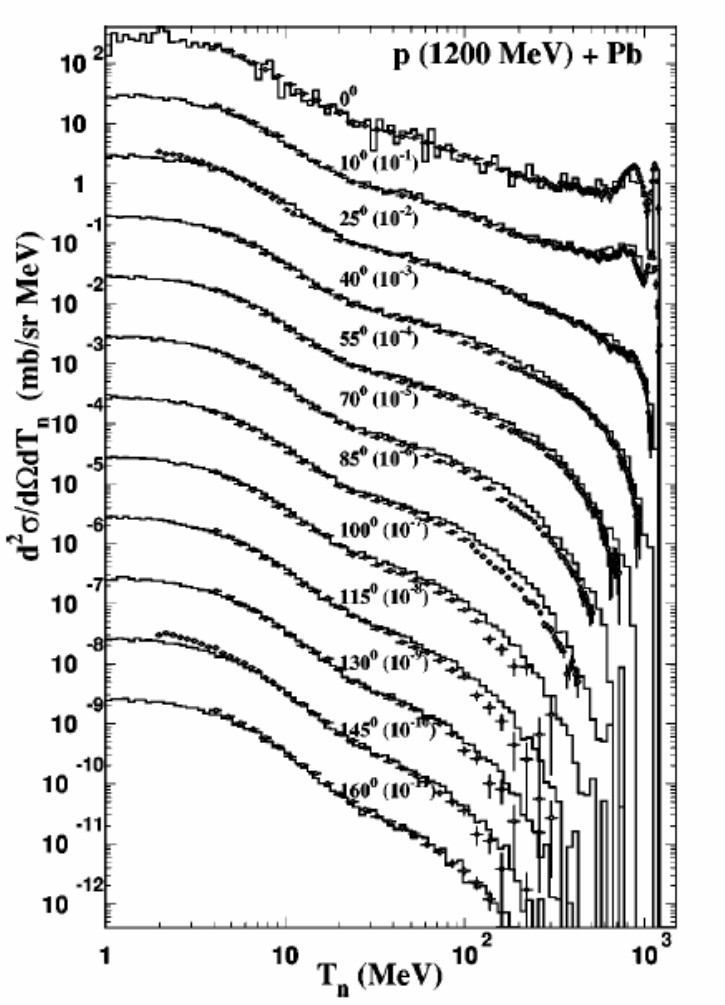

Figure 3. Double-differential neutron spectrum measured in the bombardment of a lead target by 1.2 GeV protons (data points). The histogram shows the result of a model calculation with the INCL3 code coupled to the ABLA code. (Figure taken from ref. [14].)

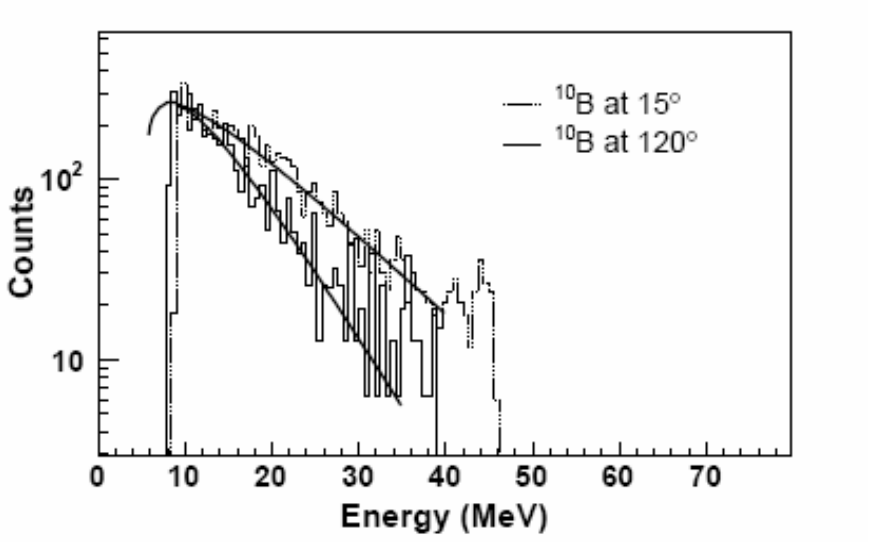

Figure 4. Energy spectra of ^{10}B isotopes from 1.9 GeV p+Ni reaction observed at 15° and 120°. The solid lines are moving-source fits. (Figure taken from ref. [15].)

The direct-kinematics approach has a severe drawback: As can be seen in Figure 3 and Figure 4, the energy spectra suffer from a lower threshold. For the investigation of heavy residues, this problem is particularly severe, because most of them do not even escape from the target. Therefore, information on the residue production was obtained by recording after irradiation the gamma activity accumulated in the target. With this technique the direct production of only a few nuclides can be measured. The activities of most nuclei represent cumulative yields, which include the intensities of several beta-decay precursors. Nevertheless, these experiments are well adapted to measure full excitation functions of specific nuclei over a large energy range [16, 17]. These can be determined in one experiment by using thick target-catcher stacks. An example is shown in Figure 12 in section 4.2.

Inverse kinematics

Using the installations of GSI, Darmstadt the reaction kinematics could be inverted. The nucleus of interest was used as a projectile, impinging on a liquid hydrogen target. This novel experimental approach allowed for the first time to identify all reaction residues in-flight. It also gives direct access to the reaction kinematics without any low-energy threshold in the projectile frame.

GSI, Darmstadt, the major European research centre for experiments with heavy-ion beams of stable and radioactive nuclides, provides unique conditions for fundamental and applied research on a variety of subjects in nuclear physics and other fields. Even more powerful installations will be available when the FAIR facility [18] will be in operation. Optimum conditions can also be found for research on several types of nuclear data for nuclear technology, radioprotection, astrophysics and other applications. Intensive work on nuclear data is presently being made e.g. on nuclear masses [19], half lives [20], nuclide yields from low-energy fission [21], and nuclide production in spallation reactions. This latter subject that is motivated by the plans for the construction of an accelerator-driven system (ADS) and for the design of the EURISOL facility [6] will be described in more detail.

Often, systematic collections of experimental data cannot cover the full variety of data requested, and nuclear-model calculations are needed to complement the experimental data bases. This is particularly true for the nuclide production in spallation reactions with all relevant target materials and projectile energies. Therefore, also in the field of model developments for the description of spallation reactions, intensive work has been performed at the GSI laboratory, see chapter 4.

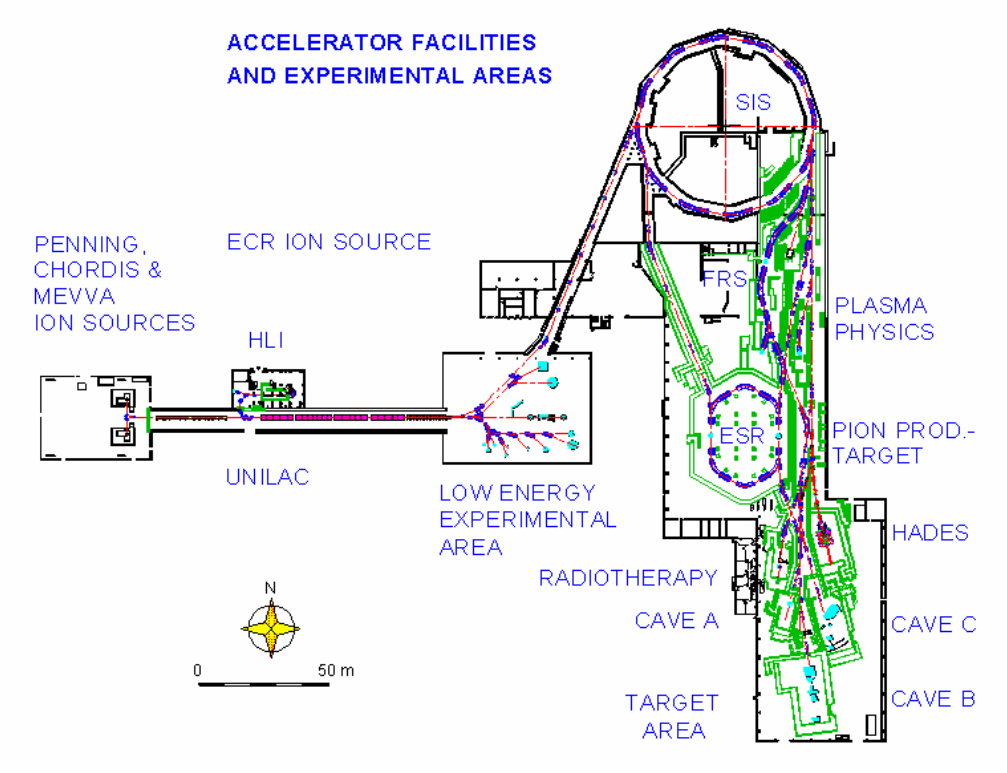

Figure 5. Installations of the GSI facility.

The basic installation of GSI is the accelerator complex with the UNILAC linear accelerator and the SIS-18 synchrotron, which is capable to provide beams of any stable nuclide up to 18 Tm, corresponding to energies of 1 *A* GeV or higher. The accelerators are complemented by the fragment

separator FRS [22], which separates the residues produced in projectile-fragmentation reactions, and thus provides a large variety of secondary beams of radioactive species in the same energy range as the primary beams.
Dedicated detectors and the large-acceptance dipole magnet ALADIN, mounted in Cave C, as well as the storage ring ESR are important experimental installations for the research on nuclear data.
Since several years, an experimental campaign is being pursued in a French-Spanish-German collaboration on measuring the individual nuclide yields in spallation reactions for a number of key reactions. For this purpose, the fragment separator is used as a high-resolution magnetic spectrometer, see Figure 6. All spallation residues are identified in nuclear charge *Z* and mass number *A*. In addition, their velocity distributions are determined, which are sensitive to the production mechanism.

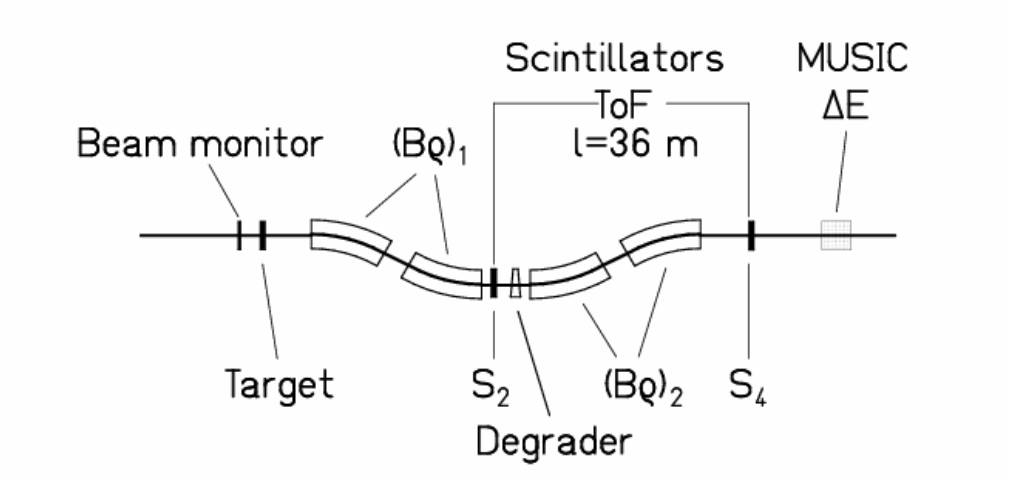

Figure 6. Schematic view of the fragment separator and the most important detector equipment.

The spallation reactions of a series of projectiles have been studied over an energy range between 0.2 and 2 GeV, counted in the frame of the heavy projectile, see table 3. The measured nuclide cross sections at the energy of 1 GeV are shown in Figure 7. Some systematic trends can be observed. While fission is dominant for ^{238}U, it contributes only little for ^{208}Pb and practically disappears for the lighter systems. The spallation-evaporation residues mostly populate the elements close to the projectile and die out around 15 elements below. When covered in the experiment, also sizeable production of light and intermediate-mass fragments is observed, revealing the continuous population of all elements below the projectile. Also some production up to two elements above the projectile by charge-pickup reactions is observed.

Table 3. List of key reactions studied at the fragment separator of GSI, Darmstadt.

projectile	target	energy in projectile frame	references
^{238}U	p, d	1 GeV, 2 GeV	[23, 24, 25, 26, 27, 28, 29]
^{208}Pb	p, d	0.5 to 2 GeV	[30, 31, 32, 33, 34, 35]
^{197}Au	p	0.8 GeV	[36, 37]
^{136}Xe	p	0.2 to 1 GeV	[38]
^{56}Fe	p, d	0.3 to 1.5 GeV	[39, 40]

The longitudinal velocity distributions of these fragments were determined as well with high precision. Figure 8 shows the result for light fragments produced with a ^{136}Xe beam. By including data measured with heavier targets, the variation of these distributions over a large range of bombarding energy in the centre-of-mass system could be studied.

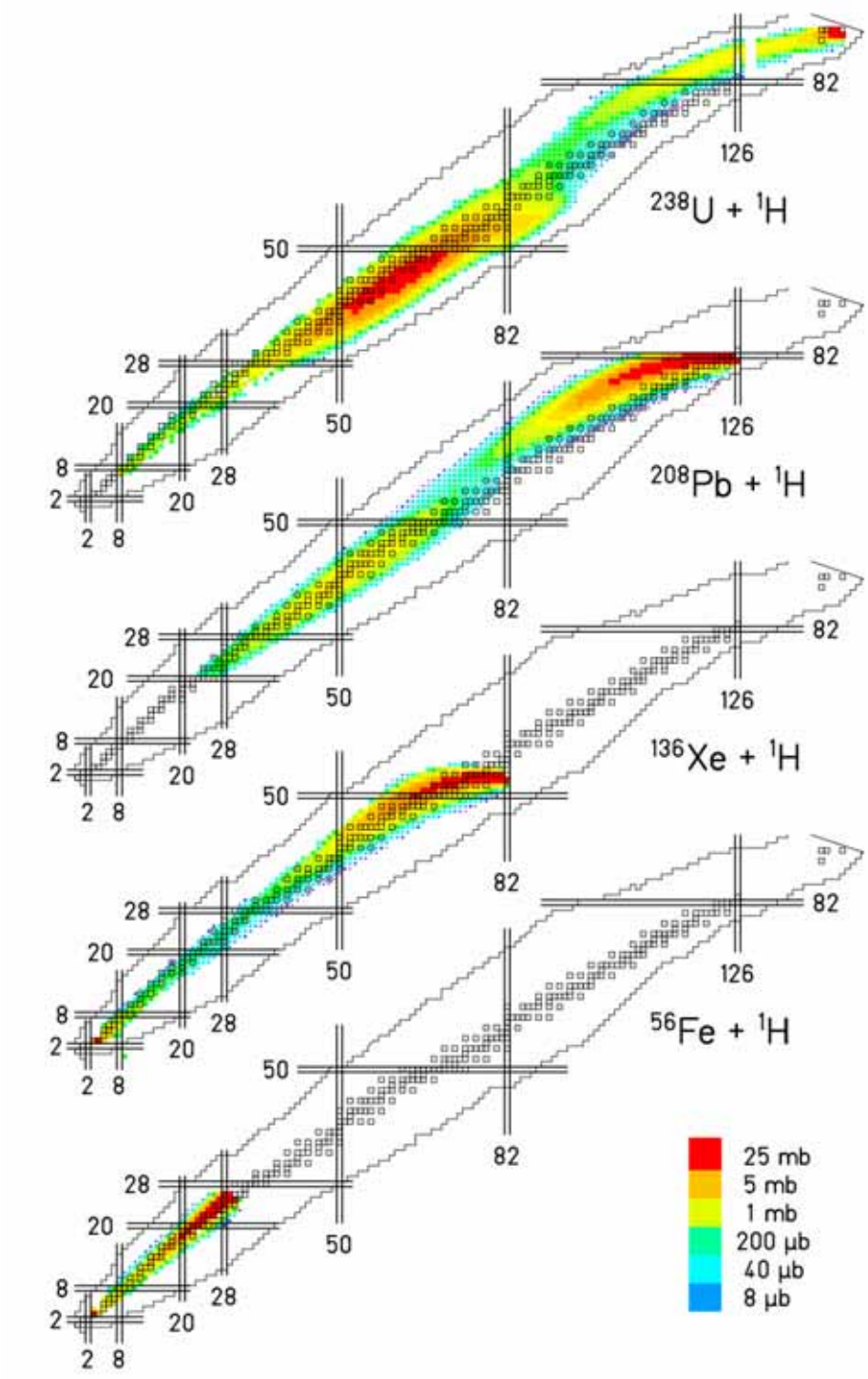

Figure 7. Overview on the nuclide production cross sections measured at the fragment separator for the four systems indicated at the energy of 1 *A* GeV on a chart of the nuclides. The colours indicate the production cross sections as defined in the colour scale.

The measured longitudinal velocity distributions for these light and intermediate-mass fragments have characteristic shapes, consisting of a double-humped and a single-humped component. The relative weight of the double-humped distribution, which is consistent with a binary decay of a heavy system close to the projectile, decreases with increasing bombarding energy and increasing fragment mass. The single-humped distribution is consistent with a multifragmentation process. Thus, the longitudinal velocity distributions allow distinguishing these two processes, which both populate the lower part of the U-shaped mass distribution. See Ref. [41] for details.

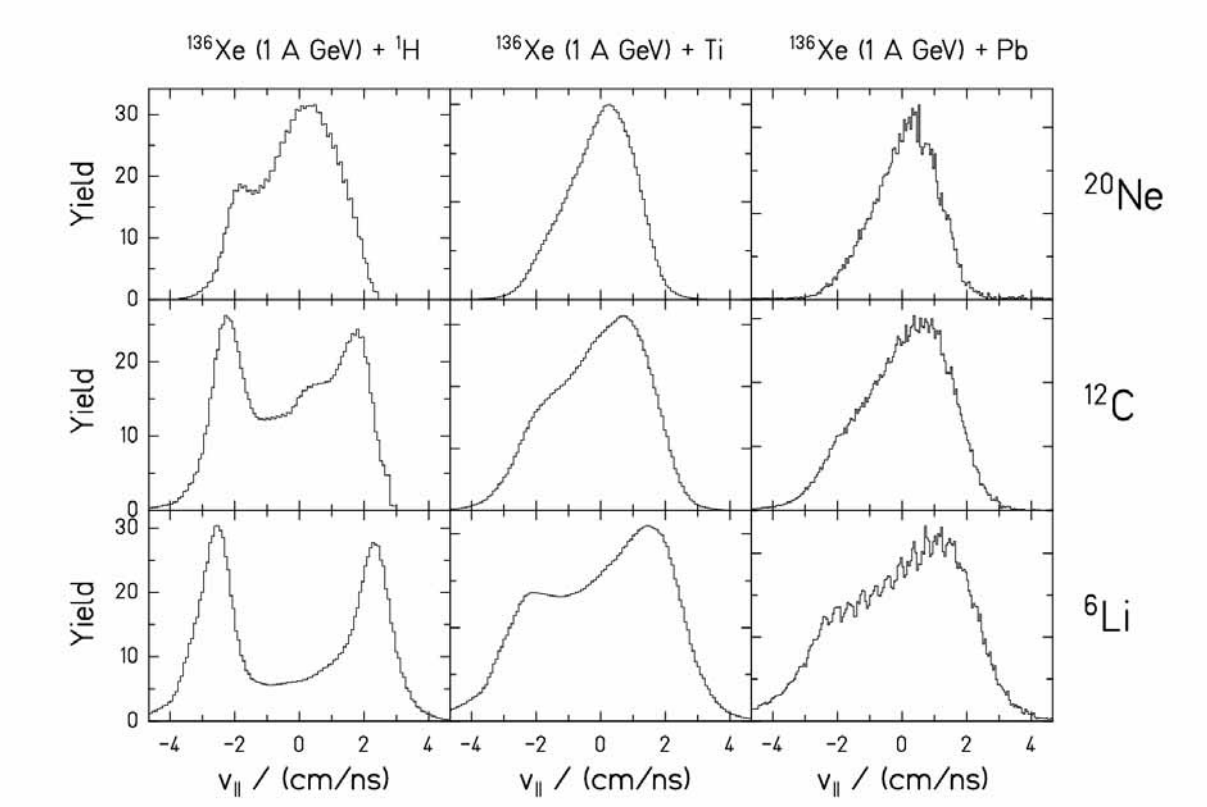

Figure 8. Longitudinal velocity distributions of light projectile fragments in the projectile frame emitted with transversal angles below 15 mr [38, 42]. The centre-of-mass kinetic energies of the three systems indicated are 1, 35.5 and 82.2 GeV, respectively.

The angular acceptance of the fragment separator covers all or at least great part of the spallation-evaporation residues. Spallation-fission products, however, are only transmitted when the fission direction is close to the beam direction, and thus the transmission losses are important. Therefore, a full-acceptance set-up was used to determine the total spallation-fission cross sections with higher precision [43], see Figure 9.

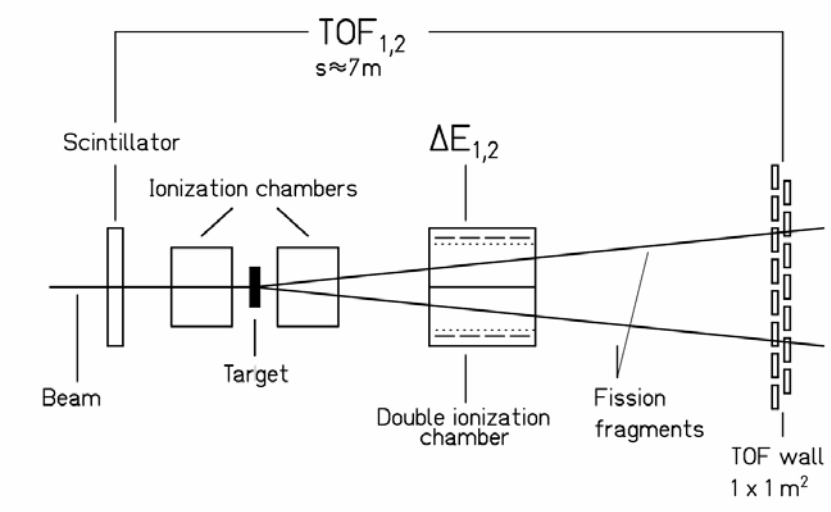

Figure 9. Set up for full-acceptance measurements of total spallation-fission cross sections.

The target is surrounded by two ionization chambers that allow discriminating reactions in other layers than the hydrogen target. The double ionization chamber and the TOF wall register the two fission fragments in coincidence.

The available results are compared in table 4 with the systematics of Prokofiev [44], and with a recent elaborate experiment [45] performed in normal kinematics. The sum of the individual fission-fragment cross sections measured at the FRS for $^{238}U+^{1}H$ are consistent with the full-acceptance results, while there is a discrepancy for $^{208}Pb+^{1}H$, which is not yet understood.

Table 4. Total fission cross sections in mb determined with the full-acceptance set up compared with previous results. The energy is given in the frame of the heavy nucleus.

reaction	full-acceptance set up [43]	FRS	Prokofiev [46]	Kotov et al. [47]
$^{208}Pb+^{1}H$ 500 MeV	146±7	232±33 [30]	112	
$^{208}Pb+^{2}H$ 1000 MeV	203±9			
$^{238}U+^{1}H$ 545 MeV	1490±100		1360	1491±78 *)
$^{238}U+^{1}H$ 935 MeV	1550±100	1530±200 [23] *)	1270	1489±64 *)

*) The beam energies were slightly different than indicated.

Recently, the SPALADIN set up has been developed, allowing for the detection of heavy spallation residues in coincidence with light particles [48]. The SPALADIN set up (Figure 10) is based on the large-acceptance dipole magnet (ALADIN) coupled with a multitrack and multisampling time projection chamber (TPC MUSIC IV).
This more exclusive experiment aims to separate the intra-nuclear cascade phase from the de-excitation phase of the spallation reaction.

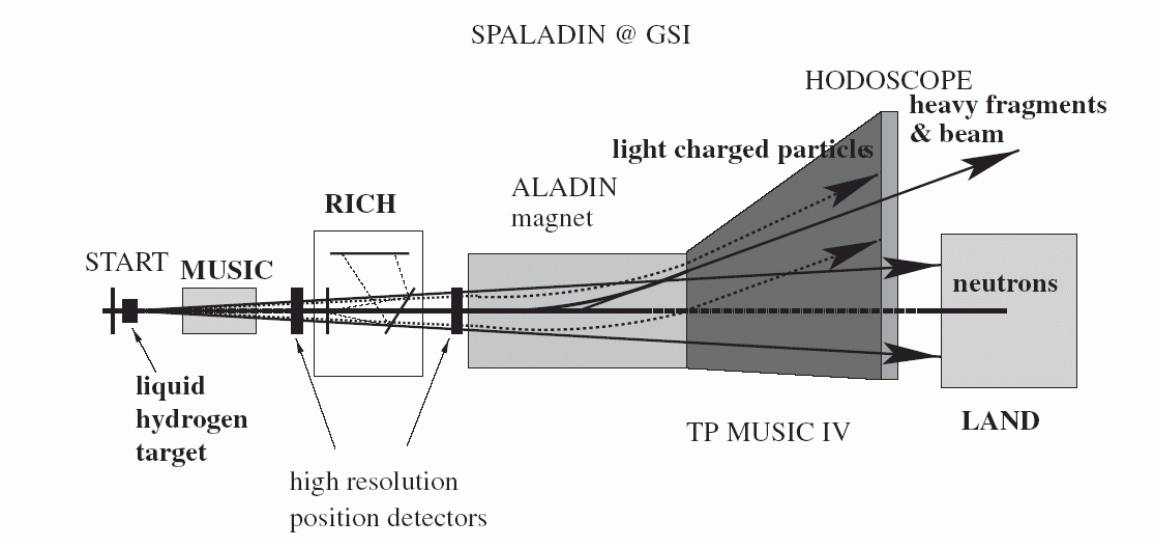

Figure 10. Schematic view on the SPALDIN experimental set up.

Physics and Models

Nuclear collisions stage

The first stage of the spallation reaction, characterized by a cascade of quasi-free nucleon-nucleon collisions, is most often described by an intra-nuclear cascade code. The nucleons of projectile and target are treated as classical objects, interacting with their respective scattering cross sections. This treatment is justified by the small de-Broglie wavelength of high-energetic nucleons: The wavelength of a 1 GeV nucleon is 0.73 fm, which is small compared to the size of a nucleus and still smaller than the average distance between two nucleons in the nucleus. Several effects, not compatible with the collision of classical objects, are incorporated in modern versions of intranuclear-cascade codes, e.g.

cluster production [49], Pauli blocking [50], and creation of pions [51]. Modern versions of the intra-nuclear cascade code extended their validity range to lower energies [52, 53] and are able to treat the nucleon-nucleon-collision stage long enough until thermal equilibrium is reached [14]. Thus, they can directly be coupled to a statistical de-excitation code. Early, less elaborate versions were able to treat the first high-energetic nucleon-nucleon collisions only and needed to be followed by pre-equilibrium models [54, 55] to describe the thermalization process.
The intra-nuclear-cascade stage – and eventually the pre-equilibrium-stage – of a spallation reaction is directly responsible for the emission of high-energetic nucleons and light fragments. It also sets the initial conditions – mass loss, excitation energy, angular momentum of the pre-fragments – for the consecutive statistical de-excitation stage. Most features observed in the measured yields of heavy residues are strongly influenced by this final reaction stage.

De-excitation process
Once the single-particle degrees of freedom are thermalized, the de-excitation process of the system can be described by a statistical code. However, there are specific requirements in the application to spallation reactions. The code needs to handle a large range of excitation energies and masses. Moreover, the technical applications require predictions with a high precision, also for rare processes. In the following, we will describe ABLA as an elaborate code, which has been developed to meet these requirements.
The ABLA code, developed at GSI, has proven to be quite successful in modelling the evaporation and the major fission processes in the de-excitation stage of the spallation reaction [14]. However, the production of intermediate-mass fragments was severely underestimated [56], because very asymmetric binary emission and simultaneous break-up were not considered. These processes have been included in the new version ABLA07. Also the treatment of the dynamics of the fission process has been improved.
As already discussed by Moretto [57], there is a finite probability for binary mass splits covering the mass range between the major, predominantly symmetric fission, and the evaporation of nucleons and light charged particles. The characteristics of these processes is a continuous transition between evaporation and fission. Previous approaches treat these processes either as very asymmetric fission (e.g. GEMINI [58]) or as evaporation of fragments (e.g. GEM2 [59]). In the new version of the code (ABLA07), an extension of evaporation to higher masses, up to the Businaro-Gallone maximum has been implemented. The emission barriers are based on a realistic nuclear potential [60], leaving no adjustable parameter. In addition, the angular momentum is treated explicitly in the evaporation process. More details can be found in refs. [26].
If the excitation energy of a system exceeds a certain limit, the yields of intermediate-mass fragments increase, and the emission times are too short to be compatible with the assumption of sequential emission [61, 62]. Also the kinematic properties clearly show specific features (see Figure 8). Different theoretical approaches and the experimental data are consistent with a mass distribution following a power law. Simultaneous break-up has been implemented in ABLA07 for initial excitation energies above $E/A \approx 3$ MeV following this idea. This value can easily be reached e.g. in the spallation of light nuclei like iron by 1 GeV protons. The fragments are produced with a freeze-out temperature of 5.5 MeV.
A good description of the fission process for many systems in an extended region of the chart of the nuclides and over a large excitation-energy range is mandatory for a realistic prediction of spallation-fission residue cross sections, because they result from a superposition of many fissioning systems. The treatment of fission dynamics has been implemented in a more consistent way. More details are given in ref. [63]. The initial deformation of the pre-fragment after the INC phase is considered when calculating the fission transients. This leads to appreciably shorter fission delays in the spallation-fission reactions of nuclei with prolate deformation. Particle emission on the path from saddle to scission and after scission are calculated explicitly. The macroscopic-microscopic approach developed in ABLA, which models the influence of shell effects on the fission process, has been refined. The features of multi-modal fission of all actinides from energies around the fission barrier up to higher energies, at which shell effects disappear, are well described with a common set of parameters. More details are given in ref. [64].
As a benchmark, the nuclide distributions of the systems shown in Figure 7 are compared in Figure 11 with ABRABLA07. In this code, the collision phase is described in the abrasion formalism. The results demonstrate a high degree of similarity with the experimental data. The features of spallation-evaporation residues, spallation-fission products and intermediate-mass fragments, mostly determined by ABLA07, resemble the experimental results. It may be concluded that the variations of the nuclide yields with the mass of the system are well reproduced by ABRABLA07.

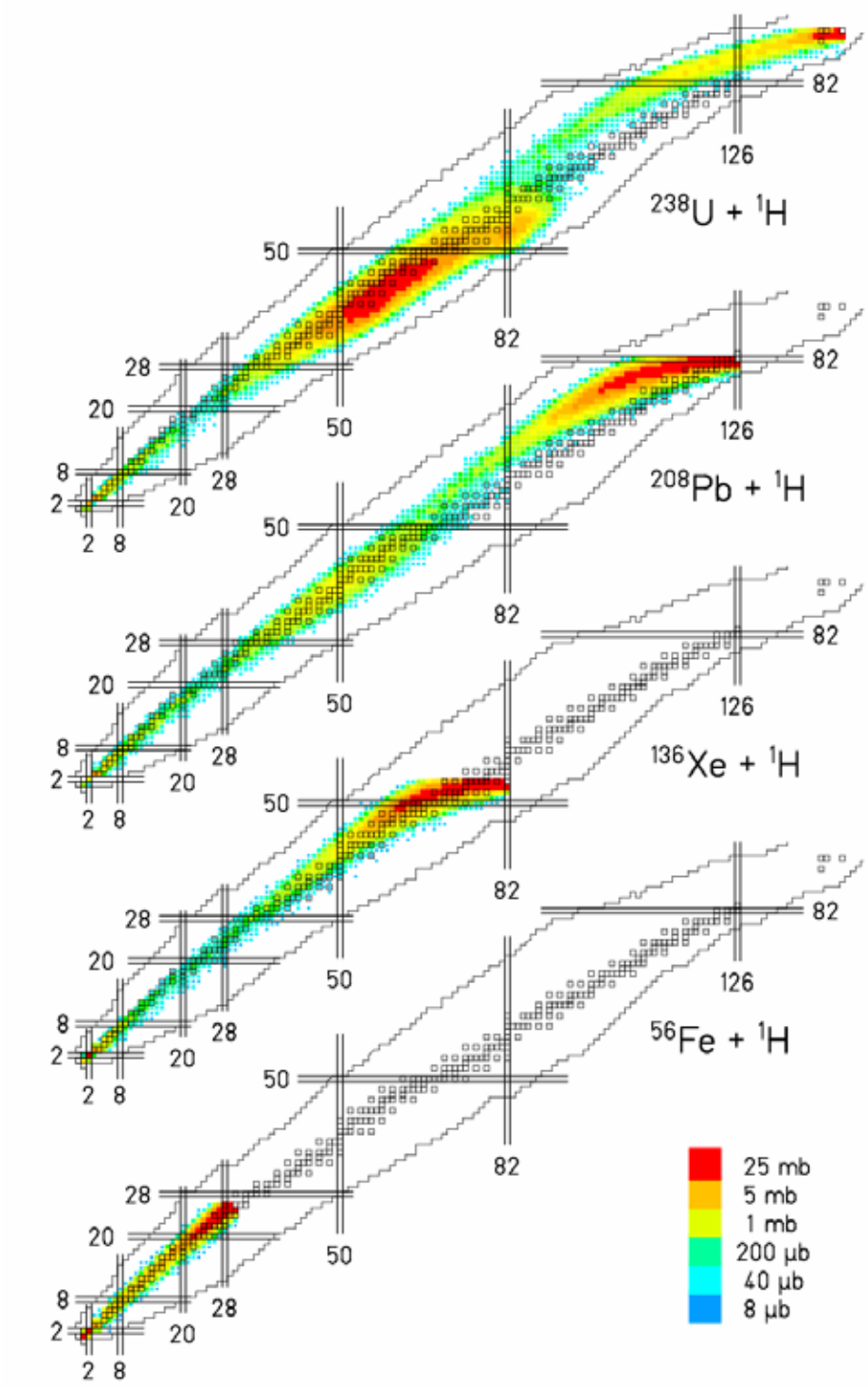

Figure 11. Overview on the nuclide production cross sections calculated with ABRABLA07 for the four systems indicated at the energy of 1 *A* GeV on a chart of the nuclides. The colours indicate the production cross sections as defined in the colour scale.

The calculated variation of the spallation process with bombarding energy can be compared with excitation functions of specific nuclides measured in activation experiments, which cover a large energy range with an important number of steps. Such a comparison has been performed by Titarenko et al. [16], proving that already the previous version of ABLA reproduced the heavy spallation products and the yields in the main fission region with good quality.

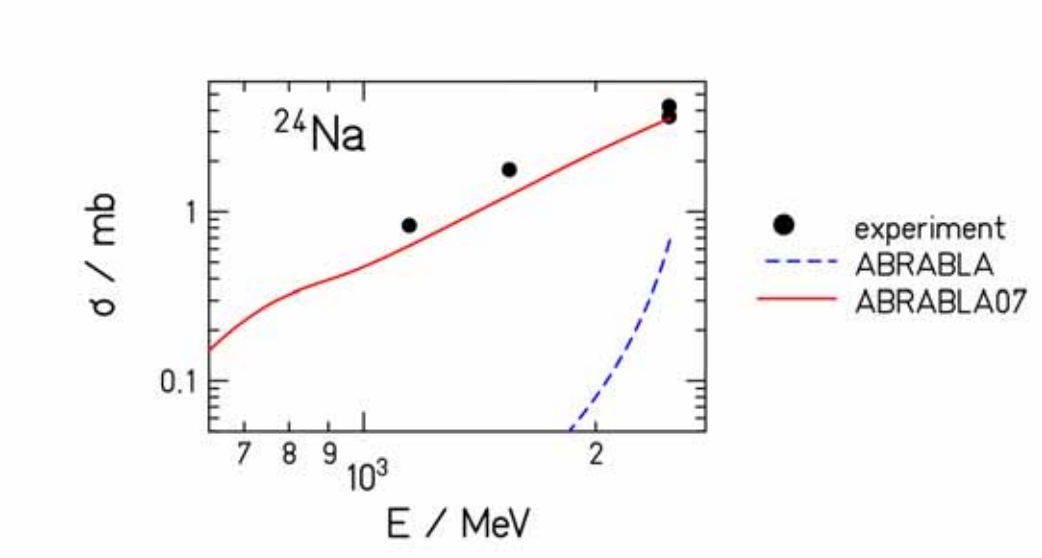

Figure 12. Measured excitation function of ^{24}Na produced in the reaction ^{209}Bi + p [16] compared with the previous ABRABLA version and the new code ABRABLA07.

Figure 12 gives a closer view on the threshold behaviour in the production of intermediate-mass fragments by comparing the excitation function of ^{24}Na from the reaction ^{209}Bi + p, measured by gamma-spectroscopy [16], with the previous and the new version of ABRABLA. Obviously, including the production of intermediate-mass fragments by evaporation and simultaneous break-up has essentially improved the agreement with the data in this mass range.

Conclusion and outlook

New interest emerged in spallation reactions due to their implications in specific astrophysical processes and as a tool to deduce the properties of nuclear matter. Moreover, there are several technical applications which ask for precise data on particle and residue production.
Answering these needs, a comprehensive program on experiments and model developments on spallation reactions is being executed at GSI, Darmstadt. A systematic set of full nuclide distributions has been obtained using the fragment separator as a high-resolution spectrometer. These experiments are complemented by full-acceptance fission experiments and more exclusive experiments emphasizing the detection of lighter fragments.
Progress in modelling the different processes of the spallation reaction has been achieved. The realistic descriptions of spallation-evaporation and spallation-fission have been complemented by sequential binary decay beyond the Businaro-Gallone maximum and simultaneous break-up.
The future FAIR facility [18] of GSI, Darmstadt, will provide substantially improved conditions for the research on a variety of subjects and in particular for experiments on nuclear data. The variety of secondary beams will be considerably extended. The set-up for reaction studies with radioactive beams (R3B) will combine experiments with high resolution and large acceptance. The ELISe electron-ion collider will be the first installation to provide full nuclide distributions for well defined fissioning systems.

Acknowledgements
The experimental results measured at GSI, Darmstadt, presented in this contribution have been obtained in a collaboration of CEA Saclay, IPN Orsay, CEN Bordeaux-Gradignan, and GSI Darmstadt. Background information on this experimental campaign can be found on the CHARMS Web (http://gsi.de/charms). This work has been supported by the European Union under contracts FIKW-CT-2000-00031, FI6W-516520, FI6W-CT-2004-012985, and FI6W-CT-2004-516352.

References

[1] E. Schopper, Naturw. **25** (1937) 557
[2] V. A. Karnaukov, Phys. of Part. and Nuclei **37** (2006) 165
[3] A. G. W. Cameron, Astroph. J. **587** (2003) 327
[4] ISOLDE: http://isolde.web.cern.ch/ISOLDE/
[5] TRIUMF: http://www.triumf.info/
[6] EURISOL: http://www.ganil.fr/eurisol/ , http://www.eurisol.org

[7] Institute Laue-Langevin: http://www.ill.fr/
[8] Swiss Spallation Neutron Source SINQ: http://sinq.web.psi.ch/
[9] ISIS: http://www.isis.rl.ac.uk/
[10] SNS: http://neutrons.ornl.gov/
[11] n_TOF: http://pceet075.cern.ch/
[12] Myrrha: http://www.sckcen.be/myrrha/home.php
[13] JAEA (Japan Atomic Energy Agency) R&D Review 2006, http://jolisfukyu.tokai-sc.jaea.go.jp/fukyu/mirai-en/pdf/7-1.pdf
[14] A Boudard et al. Phys. Rev. **C 66** (2002) 044615
[15] F. Goldenbaum, Proc. Intern. Workshop Nucl. Data for the Transm. Nucl. Waste, Darmstadt, 2003, ISBN 3-00-012276-1 http://www-wnt.gsi.de/TRAMU/
[16] M. Gloris et al. Nucl. Instrum. Methods **A 463** (2001) 593
[17] Yu. E. Titarenko et al., Nucl. Instrum. Methods **A 562** (2006) 801
[18] FAIR: http://www.gsi.de/fair/index.html
[19] Yu. A. Litvinov et al., Nucl. Phys. **A 756** (2005) 3
[20] T. Kurtukian et al., submitted to Phys. Rev. Lett., arXiv:nucl-ex/0711.0101
[21] K.-H. Schmidt et al., Nucl. Phys. **A 665** (2000) 221
[22] H. Geissel et al., Nucl. Instrum. Methods **B 70** (1992) 286
[23] E. Casarejos et al., Phys. Rev. **C 74** (2006) 044612
[24] J. Taieb et al., Nucl. Phys. **A 724** (2003) 413
[25] M. Bernas et al., Nucl. Phys. **A 725** (2003) 213
[26] M. V. Ricciardi et al., Phys. Rev. **C 73** (2006) 014607
[27] M. Bernas et al., Nucl. Phys. **A 765** (2006) 197
[28] J. Pereira et al., Phys. Rev. **C 75** (2007) 014602
[29] P. Armbruster et al., Phys. Rev. Lett. 93 (2004) 212701
[30] T. Enqvist et al., Nucl. Phys. **A 686** (2001) 481
[31] T. Enqvist et al., Nucl. Phys. **A 730** (2002) 435
[32] A. Kelic et al., Phys. Rev. **C 70** (2004) 064608
[33] B. Fernandez et al., Nucl. Phys. **A 747** (2005) 227
[34] L. Audouin et al., Nucl. Instrum. Methods **A 548** (2005) 517
[35] L. Audouin et al., Nucl. Phys. **A 768** (2006) 1
[36] F. Rejmund et al., Nucl. Phys. **A 683** (2001) 540
[37] J. Benlliure et al., Nucl. Phys. **A 683** (2001) 513
[38] P. Napolitani et al., Phys. Rev. **C** (accepted), arXiv:nucl-ex/0706.0646
[39] C. Villagrasa-Canton et al., Phys. Rev. **C 75** (2007) 044603
[40] P. Napolitani et al., Phys. Rev. **C 70** (2004) 054607
[41] P. Napolitani, K.-H. Schmidt, L. Tassan-Got (to be published)
[42] D. Henzlova et al., (to be published)
[43] K.-H. Schmidt et al., Nucl. Phys. **A** (to be published)
[44] A. V. Prokofiev, Nucl. Instrum. Methods **A 463** (2001) 557
[45] A. A. Kotov et al., Phys. Rev. **C 74** (2006) 034605
[46] A. V. Prokofiev, Nucl. Instrum. Methods **A 463** (2001) 557
[47] A. A. Kotov et al., Phys. Rev. **C 74** (2006) 034605
[48] E. Le Gentil et al., Nucl. Instrum. Methods **A 562**, 743 (2006)
[49] A.Boudard et al., Nucl Phys. **A 740** (2004) 195
[50] Th. Aoust et al., Nucl. Instrum. Methods, **A 562** (2006) 810
[51] Th. Aoust et al., Phys. Rev. **C 47** (2006) 064607
[52] J. Cugnon et al., Eur. Phys. J. **A 16** (2003) 393
[53] H. Duarte, Phys. Rev. **C 75** (2007) 024611
[54] C. Kalbach, Phys. Rev. **C 73** (2006) 024619
[55] F. Sébille et al., Nucl. Phys. **A 792** (2007) 313
[56] S. Leray et al., Nucl. Instrum. Methods **A 562** (2006) 806
[57] L. G. Moretto, Nucl. Phys. **A 247** (1975) 211
[58] R. J. Charity et al., Nucl. Phys. **A 483** (1988) 371
[59] S. Furihata, Nucl. Instrum. Methods **B 171** (2000) 251
[60] R. Bass, Lect. Notes in Phys. **117** (1980) 281
[61] S. Yu. Shmakov et al., Phys. Atom. Nuclei **58** (1995) 1635
[62] L. Beaulieu et al., Phys. Rev. Lett. **84** (2000) 5971
[63] B. Jurado et al., Nucl. Phys. **A 747** (2005) 14
[64] K.-H. Schmidt et al., arXiv:nucl-ex/0711.3967